THE JOURNAL OF BIOLOGICAL CHEMISTRY VOL. 285, NO. 42, pp. 32282–32292, October 15, 2010

Anionic Phospholipid Interactions of the Prion Protein N Terminus Are Minimally Perturbing and Not Driven Solely by the Octapeptide Repeat Domain*

Received for publication, March 14, 2010, and in revised form, July 22, 2010 Published, JBC Papers in Press, August 2, 2010, DOI 10.1074/jbc.M110.123398

Martin P. Boland[‡§], Claire R. Hatty[¶‖], Frances Separovic[**], Andrew F. Hill[§‡‡§§1], Deborah J. Tew[‡§‡‡], Kevin J. Barnham[‡§‡‡1], Cathryn L. Haigh[‡§], Michael James[¶¶¶], Colin L. Masters[§], and Steven J. Collins[‡§1,2]

*From the [‡]Department of Pathology, [§]Mental Health Research Institute, **School of Chemistry, [‡‡]Bio21 Molecular Science and Biotechnology Institute, and [§§]Department of Biochemistry and Molecular Biology, University of Melbourne, Parkville 3010, the [¶]Bragg Institute, Australian Nuclear Science and Technology Organisation, Lucas Heights, New South Wales 2234, the [‖]Faculty of Health Sciences, University of Sydney, Lidcombe, New South Wales 2141, and the [¶¶]School of Chemistry, University of New South Wales, Kensington, New South Wales 2052, Australia*

Although the N terminus of the prion protein (PrP^C) has been shown to directly associate with lipid membranes, the precise determinants, biophysical basis, and functional implications of such binding, particularly in relation to endogenously occurring fragments, are unresolved. To better understand these issues, we studied a range of synthetic peptides: specifically those equating to the N1 (residues 23–110) and N2 (23–89) fragments derived from constitutive processing of PrP^C and including those representing arbitrarily defined component domains of the N terminus of mouse prion protein. Utilizing more physiologically relevant large unilamellar vesicles, fluorescence studies at synaptosomal pH (7.4) showed absent binding of all peptides to lipids containing the zwitterionic headgroup phosphatidylcholine and mixtures containing the anionic headgroups phosphatidylglycerol or phosphatidylserine. At pH 5, typical of early endosomes, quartz crystal microbalance with dissipation showed the highest affinity binding occurred with N1 and N2, selective for anionic lipid species. Of particular note, the absence of binding by individual peptides representing component domains underscored the importance of the combination of the octapeptide repeat and the N-terminal polybasic regions for effective membrane interaction. In addition, using quartz crystal microbalance with dissipation and solid-state NMR, we characterized for the first time that both N1 and N2 deeply insert into the lipid bilayer with minimal disruption. Potential functional implications related to cellular stress responses are discussed.

Prion diseases (also known as transmissible spongiform encephalopathies) include a diverse group of neurodegenerative disorders that share a number of unifying features, including salient neuropathological changes and transmissibility. Creutzfeldt-Jakob disease, fatal familial insomnia, and Gerstmann-Sträussler-Scheinker syndrome constitute the more common human disorders, and scrapie in sheep and goats, bovine spongiform encephalopathy, and chronic wasting disease of mule deer, elk, and moose are the predominant animal forms of prion disease (1). A key event in prion disease pathogenesis is the misfolding of the normal form of the prion protein (PrP^C)[3] into isomeric, typically protease-resistant β-sheet rich conformers (designated PrP^{res}), with the latter also posited to predominantly, or perhaps exclusively, constitute the transmissible agent ("prion") (2). According to the protein-only hypothesis of propagation, PrP^{res} recruits and converts natively folded PrP^C into *de novo* PrP^{res} via an autocatalytic process (2).

Mature, full-length mouse PrP^C (moPrP) is a 208-residue variably *N*-linked glycosylated protein, attached to the outer membrane leaflet via a C-terminal glycosylphosphatidylinositol (GPI) anchor (3). Similar to other proteins, the GPI anchor is important for directing PrP^C to detergent-resistant microdomains (DRM; also known as lipid "rafts"), although the N terminus of PrP^C has also been shown capable of independently performing this function (4, 5). Structural analyses of unglycosylated, non-GPI-anchored mammalian PrP^C from various species, when analyzed in aqueous environments, have demonstrated a globular C-terminal region, dominated by three α-helical regions, two of which are linked through a disulfide bridge; the N-terminal region, encompassing residues 23 to ~125, appears largely unstructured (6). The N terminus of PrP^C can be construed as composed of three sequential subdomains as follows: a polybasic, charged glycosaminoglycan binding region (residues 23–50; unless otherwise stated, all references to amino acid sequences are to murine PrP) (7); an octapeptide (PHGGGWSQ) repeat domain, with hydrophobic and copper-binding properties (8); and a hydrophilic, copper binding domain (approximately residues 90–110) (9), which also

* This work was supported in part by an Australian Nuclear Science and Technology Organisation/University of Melbourne collaboration grant.
[1] Supported by National Health and Medical Research Council fellowships with further funding from National Health and Medical Research Council Program Grant 400202.
[2] To whom correspondence should be addressed. Fax: 613-9349-5105; E-mail: stevenjc@unimelb.edu.au.

[3] The abbreviations used are: PrP^C, cellular prion protein; moPrP, mouse PrP^C; LUV, large unilamellar vesicle; SUV, small unilamellar vesicle; POPC, 1-palmitoyl-2-oleoyl-*sn*-glycero-3-phosphocholine; POPG, 1-palmitoyl-2-oleoyl-*sn*-glycero-3-phospho-(1′-*rac*-glycerol); POPS, 1-palmitoyl-2-oleoyl-*sn*-glycero-3-phospho-L-serine; QCM-D, quartz crystal microbalance with dissipation; GPI, glycosylphosphatidylinositol; DRM, detergent-resistant microdomain; MLV, multilamellar vesicle; LPC, 1-(9*Z*-octadecenoyl)-*sn*-glycero-3-phosphocholine; CSA, chemical shift anisotropy; MAS, magic angle spinning; PS, phosphatidylserine; PG, phosphatidylglycerol.

appears to have some capacity to bind glycosaminoglycans albeit with lesser affinity (10).

As part of its normal cellular biology, PrP^C, upon binding Cu^{2+} (11) and/or Zn^{2+} (12), can exit DRMs and move laterally though detergent-soluble membrane zones to allow endocytosis mediated by clathrin-coated pits (13), with the polybasic region (residues 23–28) essential for this trafficking (14, 15). In addition, PrP^C can be cleaved near its C terminus or within the GPI anchor and be secreted or "shed" into the extracellular milieu (16, 17). As for the cell-associated trafficking of PrP^C, the significance of shedding is poorly understood, but it clearly liberates PrP^C to potentially participate in membrane associations not readily available to it while tethered through a GPI anchor at its C terminus.

Notably, PrP^C can undergo two constitutive cleavage events, with their true biological significance yet to be fully elucidated. Cleavage between residues 109/110 or 110/111, α-cleavage (18), gives rise to the N1 (23–110/111) and C1 (110/111–231) fragments. Alternatively, cleavage around residue 90, β-cleavage, produces the N2/C2 combination (19).

A complete understanding of the molecular basis and cellular location of PrP^C to PrP^{res} conversion remains elusive as does the normal function of PrP^C. Several biomolecules have been implicated in the structural conversion of PrP^C into its pathogenic isoform. These include RNA (20), transition metals such as copper, zinc, and manganese (21), glycosaminoglycans (22), and membrane-associated lipids, with the latter potentially serving as a platform to facilitate structural transitions (23, 24). Interactions of soluble PrP^C with the core of the lipid bilayer have also been proposed as directly contributing to prion-mediated neurotoxicity (25). In addition to these likely deleterious associations, there are less explored interactions between PrP^C and membrane lipids, which may be important for either controlling or subverting normal physiological activities. Certainly, induced membrane lipid perturbations can unfavorably influence protective properties and intracellular signaling associated with PrP^C processing or cognate peptide exposure (26, 27). Localization of proteins to the exoplasmic face of DRMs through a GPI anchor is often associated with receptor or cell-signaling properties, with evidence to support this function for PrP^C (28, 29).

Extending the lipid associating capacity of PrP^C independent of the GPI anchor, PrP(23–145) and full-length PrP^C have both been shown to also bind to model non-DRM lipid membranes, specifically to small unilamellar vesicles (SUV) containing POPS (30), with greater affinity at acidic pH. The specificity of the membrane lipid binding is of interest. No binding affinity was observed in relation to POPC, the dominant lipid in non-DRM membrane segments, with a consistent and significant pH-dependent association found with POPS. This contrasts with full-length hamster PrP, which was shown to be capable of binding to POPC at pH 5, suggesting there may be differing species affinities for specific phospholipids perhaps most easily appreciated for the restricted regions of the prion protein (31). Anionic lipids such as POPS and POPG are expressed in low quantities compared with bulk phospholipids such as POPC. However, these charged lipids have been associated with functional roles such as mediating intracellular signaling (32), promotion of phagocytosis (33), and induction of changes to the outer face of the lipid membrane (34), including those preceding the formation of endocytic pits (35). These observations are consistent with the hypothesis that it is these minor phospholipid species that determine meaningful biological activities, such as protein activation or signaling processes, within a dominant but biologically inert PC membrane scaffold (36).

Preliminary studies have suggested the N terminus of PrP^C is capable of binding to non-DRM lipid membranes. However, there remain many fundamental issues, such as the precise determinants, biophysical basis, and functional relevance, especially in relation to the constitutively produced N1 and N2 fragments. Using a range of biophysical approaches, we have been able to provide novel and important insights into these fundamental questions. Through fluorescence and QCM-D studies, we were able to demonstrate for the first time that the highest affinity binding occurred with fragments equivalent to N1 and N2, selective for anionic lipid species. Of particular note, our detailed characterization of the determinants of non-DRM lipid binding underscored the need for a combination of the octapeptide repeat region and an N-terminal polybasic domain for effective membrane interactions to occur. In addition, using QCM-D and solid-state NMR, we determined that both N1 and N2 deeply insert into the lipid bilayer but with minimal disruption. As a corollary to more clearly characterizing the determinants and biophysical underpinnings of the binding of N1 and N2 peptides to model non-DRM lipid membranes, we offer tentative insights into the possible biological relevance of such interactions.

EXPERIMENTAL PROCEDURES

Lipids and Synthetic PrP Peptides—All phospholipids were purchased from Avanti Polar Lipids, Alabaster, AL, and used without further modification. Synthetic N-terminal peptides based on the mouse PrP sequence were utilized in this study. These were synthesized by the Peptide Technology Laboratory, Research Transfer Facility, Bio21 Institute, University of Melbourne. The peptides are summarized in Fig. 1 and consisted of the following: PrP(23–50); PrP(23–89); PrP(23–110); PrP(51–89); PrP(50–110); PrP(23–110)Δ51–89 (*i.e.* 23–110 with the octapeptide repeat region deleted); and PrP(90–110). Peptide sequence and purity (>95%) were verified by HPLC and mass spectrometry. Full-length recombinant moPrP was also used in initial experiments as a positive control to assist optimizing conditions, with its production as described previously (37). Unless otherwise stated, the following buffers were used: for pH 5, 50 mM acetate, 100 mM NaF; and for pH 7.4, 20 mM phosphate, 100 mM NaCl.

Preparation of Lipid Vesicles—Large multilamellar vesicles (MLV) were produced from POPC or mixtures of POPC with either POPG or POPS in 2:1 and 4:1 molar ratios as described previously (38). Chloroform/methanol (9:1 v/v) was used to dissolve the lipids in a round bottom flask. The solvent was removed by rotational film evaporation to leave a thin film. Vesicles were formed by resuspending the lipid film with the appropriate buffer prior to 4–6 freeze-thaw cycles using liquid nitrogen and water at 37 °C.

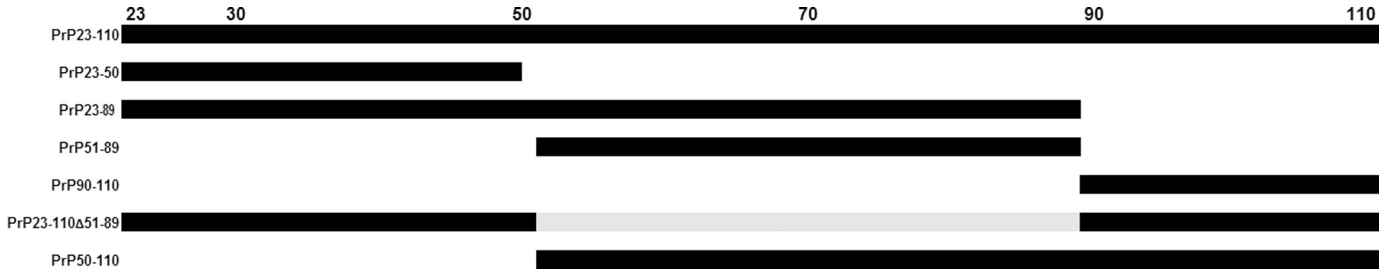

FIGURE 1. **Schematic illustration of the N-terminal region of mouse PrP encompassing residues 23–110, with the various peptides utilized in the study depicted below.** The peptides used in this work are schematically represented by the *black bars*. The *gray region* shows the residues deleted from the PrP(23–110)Δ51–89 peptide.

Large unilamellar vesicles (LUV) were produced by 11 passes of the MLV suspensions though a 0.1-μm polycarbonate membrane filter (GE Healthcare) using a manual extruder (Avestin, Ottawa, Canada). LUV were stored at room temperature and used within 24 h of preparation. Small unilamellar vesicles (SUV) were produced by the sonication method of Koenig *et al.* (39)

Fluorescence Spectroscopy—Intrinsic tryptophan fluorescence of the peptides was measured using either a Thermo-Electron Varioskan multimode plate reader equipped with onboard liquid dispenser, a Varian Eclipse spectrophotometer, or a Cary 100 fluorimeter using 1-cm path length quartz cuvettes. For plate reader experiments, initial peptide concentrations were 12.5 μM. Fluorescence was excited at 295 nm, and a spectrum was recorded between 315 and 460 nm. A point was recorded every 1 nm with an averaging time of 200 ms. Effects of dilution on the samples were accounted for in the analysis of the spectral data.

Circular Dichroism—A Jasco 810 spectropolarimeter was used to record CD spectra with wavelength analyses between 195 and 260 nm. Samples at 15 μM peptide in the appropriate buffer were contained in a 0.1-cm path length quartz cuvette, with all experiments conducted at room temperature. Background spectra (buffer or LUV solution) were subtracted from the peptide spectra.

Solid-state NMR—All solid-state NMR experiments were preformed on a Varian Inova-300 spectrometer (Palo Alto, CA) using a 5-mm Doty (Columbia, SC) magic angle spinning (MAS) probe at 30 °C. Experiments and analysis were adapted from Pukala *et al.* (40). For ^{31}P experiments, the probe was tuned to a frequency of 121.5 MHz and referenced to H_3PO_4 (0 ppm). To maximize signal/noise, ^{31}P relaxation experiments were performed under MAS conditions at a spin rate of 4 kHz. The inversion recovery pulse sequence was used to measure the longitudinal relaxation time (T_1) with internal delay times 0.01–2.0 s. Transverse relaxation times (T_2) were measured using the Hahn spin-echo experiment with internal delay times of 0.2–160 ms. ^{2}H experiments were performed at 46.1 MHz using a solid-echo sequence.

Peak intensities were measured using the integration function of the VNMR software package (Varian Inc.). Peak intensity was plotted in relation to the delay time in the inversion recovery or Hahn spin-echo pulse sequences using Prism 4 (GraphPad Software Inc.) and a single exponential curve fitted to the data. The relaxation times are presented as the average of at least two experiments, and the range between the values was calculated.

NMR samples contained a 10-mg mixture of POPC/POPS (2:1) MLV prepared as described above and suspended in 100 μl of 10 mM MES, 50 mM sodium chloride, pH 5. Peptides were added to the lipid film from stock solutions to a 20:1 lipid/peptide molar ratio prior to MLV formation.

Quartz Crystal Microbalance with Dissipation—QCM-D monitoring experiments were performed in parallel using a Q-Sense E4 quartz crystal microbalance (Q-Sense AB, Frölunda, Sweden) using methods previously published (41). Briefly, AT-cut quartz crystals with a fundamental resonance frequency of 5 MHz (Q-Sense) were used. Frequency and dissipation changes were recorded at the fundamental 1st, 3rd, 5th, 7th, 9th, 11th, and 13th harmonics. Unless stated otherwise, changes to the resonance frequency (Δf) and dissipation (ΔD) reported here are those for the 7th harmonic (or 35 MHz). Experiments were performed under temperature control at 22 °C.

The dissociation constant of the peptide-lipid complex was calculated from the kinetic binding constants extracted from the frequency curve via least squares fitting of the following Equations 1 and 2 (42),

$$\Delta f = \Delta f_0 e^{-(k_{on}(t - t_0))} \quad \text{(Eq. 1)}$$

where Δf is the frequency at time t; Δf_0 is the frequency change at time t_0, and k_{off} is the off rate;

$$\Delta f = -\frac{k_{on}[P]\, f_{max}}{k_{on}[P] + k_{off}}(1 - e^{-((k_{on}[P] + k_{off})(t - t_0))}) \quad \text{(Eq. 2)}$$

where k_{on} is the on rate, [P] is the concentration of the experimental peptide, and f_{max} is the resonance frequency of the crystal at maximum coverage. Data were analyzed using the Q-Tools (Q-Sense) software. Averages for each experiment were derived from a minimum of three trials.

RESULTS

The N-terminal region of PrP^C, residues 23–110, can be arbitrarily construed as composed of three relatively distinct subdomains in relation to amino acid composition, and copper and glycosaminoglycan binding capacity (8). To model the binding affinity of the three individual N-terminal subdomains, and the potential influence of interactions between certain combinations of segments in relation to synthetic membranes, the fol-

lowing peptides based on murine PrP^C were utilized: PrP(23–50), PrP(51–89), PrP(90–110), PrP(23–89) (representative of the N2 endoproteolytic fragment), PrP(23–110) (equivalent to the N1 endoproteolytic fragment), PrP(50–110), and PrP(23–110)Δ51–89; moPrP was also used as a positive control in initial synthetic membrane binding studies.

Three mono-unsaturated diacyl phospholipids were used to probe the interactions between the peptides and lipid membranes. POPC represents the bulk phospholipid of the cell membrane, with POPS and POPG anionic lipids that have functional roles in neurons. LUV and supported bilayers were chosen as model membranes, in preference to the SUV used in previous studies (30). The metastable nature of SUV and the high degree of membrane curvature they exhibit can cause anomalous lipid-peptide interactions that are not representative of the cell membranes; LUV and supported membranes do not suffer from these issues (43). All experiments were performed above the liquid lamellar (L_α) phase transition temperature of the lipid mixtures.

Intrinsic Tryptophan Fluorescence—The aromatic amino acids tyrosine and tryptophan are fluorescent, with excitation maxima around 280 nm, with tryptophan providing the stronger emission signal. Given that PrP(23–50) and PrP(90–110) each only contain single tryptophan residues, whereas PrP(51–89) contains five, peptide concentrations were optimized to obtain the best spectra from each of the peptides (43). Under fully hydrated (polar) conditions, tryptophan has an $E_{m,\max}$ ≈350 nm, although in a hydrophobic environment $E_{m,\max}$ is shifted to a shorter wavelength. In addition, the relative fluorescence intensity of tryptophan is increased in hydrophobic media when compared with the value in a polar solvent.

The $E_{m,\max}$ values observed for moPrP and all of the synthetic peptides in buffers without added lipid at both pH 5 and pH 7.4 fell within the range 346–349 nm indicating that the tryptophan residues are in a polar environment, consistent with previous observations of full-length PrP (30) and with the expectation that the peptides are unfolded in solution (6). Incubating moPrP and the various peptides with increasing concentrations of LUV composed only of the zwitterionic POPC did not induce any consistent change to $E_{m,\max}$ or relative fluorescence intensity at either pH (Fig. 2, *A* and *D*). This indicates that moPrP (especially the N-terminal region) does not interact with the bulk lipid of the cell membrane over the physiological pH range 5–7.4. At higher lipid concentrations, there was minor binding of moPrP to POPC/POPG at pH 7.4 but no observable spectral change for any of the various PrP peptides with titration of either POPC/POPG or POPC/POPS at around neutral pH (Fig. 2, *B* and *C*). The limited affinity of moPrP for anionic lipid membranes at pH 7.4 contrasts with previous studies using wild-type human PrP, where considerable binding to SUV composed of POPC/POPS (2:1) at pH 7 was observed but with decreased affinity compared with the lower pH (30). However, it is to be stressed that our experiments were conducted using LUV rather than SUV. Therefore, this discrepancy may be caused by the smaller membrane radius of the SUV allowing easier access to the hydrophobic core of the membrane resulting in less physiologically relevant binding to SUV (44). Alternatively, the sequence difference between human and mouse PrP may be sufficient to cause a difference in affinity.

At pH 5, LUV suspensions of POPC/POPG and POPC/POPS at the molar ratio 2:1, revealed a distinct blue shift of $E_{m,\max}$ and an increase of fluorescence intensity for the spectra of moPrP, PrP(23–89), and PrP(23–110), with greater changes observed for POPC/POPG LUV (Fig. 2, *E* and *F*). The fluorescence spectra of PrP(50–110) and PrP(23–110)Δ51–89 showed no change of $E_{m,\max}$ and relative fluorescence intensity at pH 5 with both POPC/POPG and POPC/POPS LUV (Fig. 2, *E* and *F*). Intrinsic fluorescence binding experiments using PrP(23–50) and PrP(90–110) did not show a change of fluorescence intensity or $E_{m,\max}$ under any experimental conditions (data not shown). The lack of change to these parameters indicates that neither of these shorter peptides has any affinity for POPC or anionic membranes irrespective of pH. Furthermore, in parallel with the above experiments, we also screened the peptides for binding to LUV containing a 4:1 ratio of zwitterionic/anionic lipids (results not shown). In these experiments, none of the peptides showed systematic changes to either $E_{m,\max}$ or fluorescence intensity, indicating that they did not bind to the lipids. Cumulatively, these findings suggest N-terminal peptide-lipid binding will only occur under relatively specific circumstances.

Given the intrinsic net charge of segments of the various peptides, for example the polybasic region 23–28, and the anionic nature of POPG and POPS, we assessed the role of electrostatic forces in the peptide-lipid interactions. Sodium chloride titration experiments (to a final concentration of 1 M) indicated electrostatic interactions did not cause the membrane binding of the peptides (results not shown).

Quartz Crystal Microbalance with Dissipation—QCM-D monitoring is a highly sensitive gravimetric technique that is able to detect changes to mass in the subnanogram range, and it has been extensively used to study the membrane binding and disruption properties of various peptides (41). Fundamentally, alterations in the resonant frequency of the QCM-D sensor (Δf) can be related to changes in the mass of the sensor consequent to the material deposited. Fig. 3 is a sensorgram of a typical QCM-D experiment, depicted from the solution-only base line to the final wash-off of the peptide.

Subsequent to the positive results of the initial fluorescence studies, we undertook detailed QCM assessment of the binding of the synthetic peptides to supported bilayers consisting of POPC/POPS or POPC/POPG at a 2:1 ratio at pH 5 (Fig. 4). Identical experiments were also conducted with pure POPC bilayers, and consistent with the fluorescence analysis, no binding of the any of the peptides was observed (data not shown). The peptides PrP(23–89), PrP(23–110), PrP(50–110), and PrP(23–110)Δ51–89 demonstrated different levels of binding to both POPC/POPG and POPC/POPS bilayers, with PrP(23–89) and PrP(23–110) showing the greatest binding. All of the binding peptides showed greater deposition on POPC/POPG membranes. Peptides PrP(23–50), PrP(51–89), and PrP90–110 did not show significant changes to Δf (Fig. 4), indicating that they do not bind to the lipids.

All experiments showed a reproducible profile, with the sensorgram trace being consistent with SUV binding to the QCM sensor before rapidly fusing to form a stable bilayer. A wash

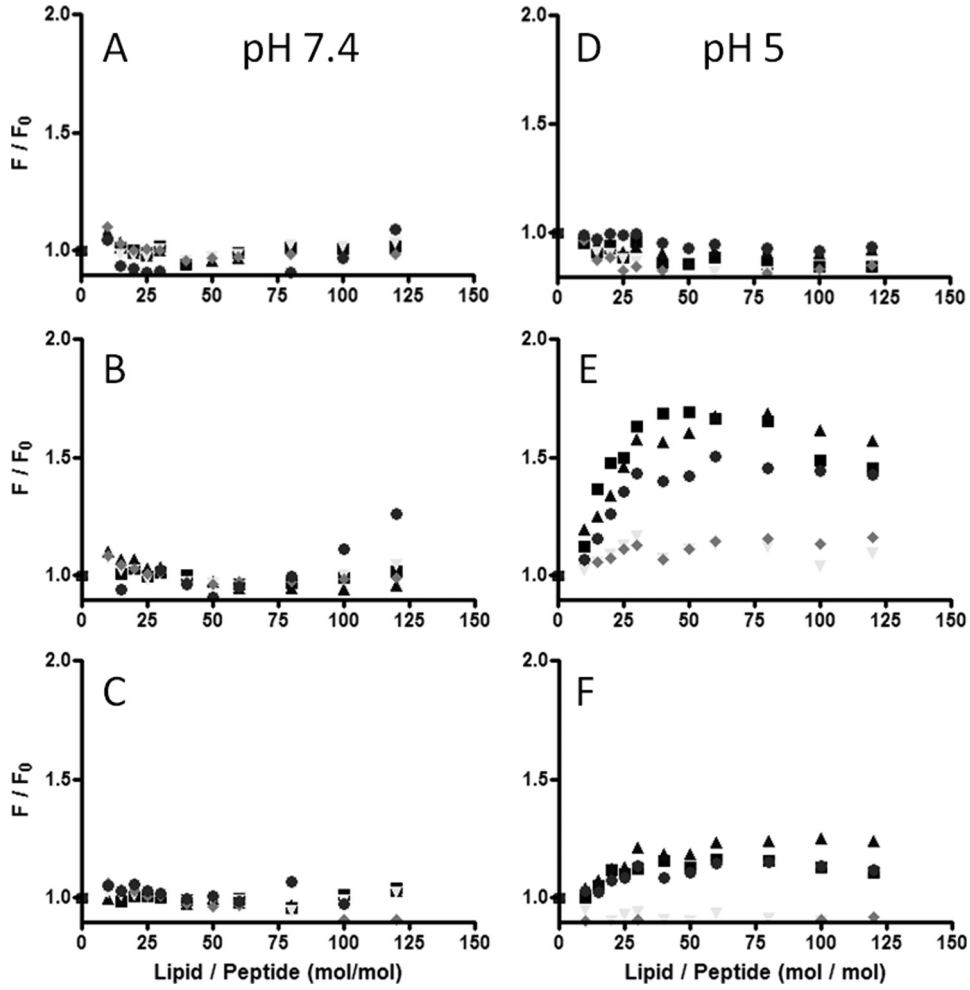

FIGURE 2. **Intrinsic tryptophan fluorescence intensity change of full-length wild type recombinant mouse PrP and various cognate N-terminal synthetic peptides in response to different LUV lipid environments.** The peptides presented are as follows: PrP(23–110) (■); PrP(23–89) (▲); PrP(50–110) (▼); PrP(23–110)Δ51–89 (♦); and recombinant moPrP (●). The panels show the results of titration as follows: *A,* POPC, pH 7.4; *B,* POPC/POPG (2:1), pH 7.4; *C,* POPC/POPS (2:1), pH 7.4; *D,* POPC, pH 5; *E,* POPC/POPG (2:1), pH 5; and *F,* POPC/POPS (2:1), pH 5. Experiments were performed at room temperature in either 50 mM sodium acetate, 100 mM NaF, pH 5, or 20 mM phosphate, 100 mM NaCl, pH 7.4. f/f_0 is the ratio of tryptophan fluorescence intensity of the peptide in the presence of LUV to the fluorescence intensity of the peptide in buffer.

with buffer caused a very small increase in Δf, indicating extraneous SUV being removed from an otherwise intact bilayer. When peptide was present, deposition was indicated by a rapid decrease in Δf before reaching a plateau. Upon starting the flow of buffer into the QCM cell, the sensorgram indicated a loss of mass from the chip. In no case was the loss of mass from the chip initiated prior to the buffer wash or was the loss greater than the increase in mass due to peptide binding. From this we suggest the loss of mass is due to the dissociation of peptide from the lipid bilayer rather than the removal of a lipid-peptide complex from the QCM sensor in a detergent-like manner.

Changes to the resonance frequency of the QCM chip at different overtones provides insight into the condition of the membrane at various distances from the chip, with higher overtones indicating activity closer to the chip surface (41). Nonetheless, in analyzing QCM-D data, it is usual to discard the first harmonic, as this senses the chip coupled molecules of the bulk solution above the chip, and thus the trace is not relevant to the behavior of the deposited lipid and peptides. In this study, we used the 3rd, 5th, 7th, 9th, 11th, and 13th overtones. All measured harmonics of the QCM chip responded in a similar way for each of the peptides for both the POPC/POPG and POPC/POPS membrane compositions. The similar effect for each overtone is consistent with the peptides inserting into the bilayer in a transmembrane manner (41). The modest difference between the 3rd and 13th harmonics for the interaction of PrP(23–110) with POPC/POPS and for each of the binding peptides with POPC/POPG suggests that a small excess of the peptide may associate with the bilayer surface only.

The amount of peptide bound to the outer leaflet of the bilayer was calculated in stoichiometric terms and expressed as the number of lipids per molecule of peptide bound (summarized in Table 1). The association rate (k_{on}) and dissociation rate (k_{off}) of the peptides can be calculated from the binding and elution phases of the QCM-D experiment (42). The calculated values of k_{on}, k_{off}, and K_d are given in Table 2.

All of the peptides that bind to the membranes have a modestly higher affinity for the POPC/POPG bilayers than for POPC/POPS and bind at a lower lipid/peptide ratio. The difference in the required number of lipid molecules was particularly noticeable for two peptides: PrP(23–110)Δ51–89, 10 for POPC/POPG compared with 20 for POPC/POPS; and PrP(50–

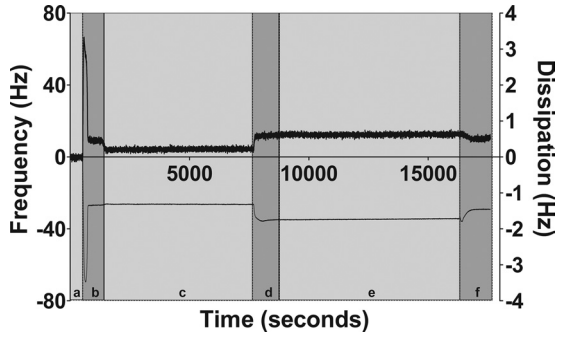

FIGURE 3. **Typical QCM-D sensorgram.** The *lower line* represents changes to the vibrational frequency of the QCM chip (Δ*f*, left-hand axis), and the *upper line* is the dissipation of energy through the adsorbed lipid (Δ*D*, right-hand axis). Progress of the experiment is delineated by alternating *light* and *dark gray shading* corresponding with the symbols *a–f*. *a,* base-line condition under acetate buffer 50 mM, pH 5, with NaCl, 100 mM; this is the condition to which changes to Δ*f* or Δ*D* are referenced. *b,* addition of lipid in the form of SUV (lipid in this example is POPC/POPS (2:1), pH 5), leading to the coating of the chip with the SUV (rapid decrease in Δ*f* to around −60 Hz) and their breaking open to form a bilayer in contact with the QCM chip (rapid increase in Δ*f* to a value around −30 Hz). *c,* wash with acetate buffer to remove extraneous SUV (slight increase in Δ*f* and decrease in Δ*D*). *d,* injection of moPrP(23–89)-peptide leading to the absorbance of the peptide to the bilayer (rapid decrease in Δ*f* to *c,* −40 Hz). *e,* incubation of peptide with bilayer with no resulting change to Δ*f* or dissipation over time, indicating that the bilayer is not disrupted by the peptide. *f,* wash with acetate buffer causing dissociation of the peptide from the lipid rapid increase in Δ*f*.

110), 20 for POPC/POPG and 80 for POPC/POPS. Each of the peptides that demonstrated binding had K_d values in the submicromolar range for membranes containing either POPS and POPG. These are composed of "on-rates" in the region of 40,000 M s^{-1} with "off-rates" around 0.004 s^{-1}. These figures would indicate that the PrP peptide-lipid complexes both associate and dissociate an order of magnitude faster than other peptides that have been studied by QCM (42).

Solid-state ^2H and ^{31}P NMR Studies—^{2}H and ^{31}P solid-state NMR of phospholipid bilayers are additional noninvasive methods to study protein-lipid interactions using deuterated phospholipids. The use of these two nuclei is complementary with ^{2}H favoring studies of the membrane hydrophobic core via the acyl chains, although ^{31}P studies probe the headgroup region of the lipids.

The NMR studies concentrated on the N-terminal peptides that show the most significant membrane binding by fluorescence and QCM-D experiments, PrP(23–89) and PrP(23–110). Furthermore, although both PrP(23–89) and PrP(23–110) bound to phosphatidylglycerol with modestly higher affinity than phosphatidylserine, we chose to undertake the NMR studies with the latter because PS is found at higher levels than PG in mammalian neural cells (45) and has been previously reported to selectively interact with other peptides such as Aβ (38, 46). Moreover, PS is found in significant amounts in the cell plasma membrane and on the surface of endosomal compartments (47), locations where PrP^C is found, whereas PG headgroups are mostly found in the mitochondrial membranes as a precursor of cardiolipin (48). Therefore, the NMR experiments were only performed with a mixture of POPC and POPS.

^{31}P Solid-state NMR—Phospholipid headgroups can be probed using ^{31}P solid-state NMR (40). In particular, the order of the headgroups can be ascertained from broad line ^{31}P NMR (49), although relaxation measurements give an insight into the

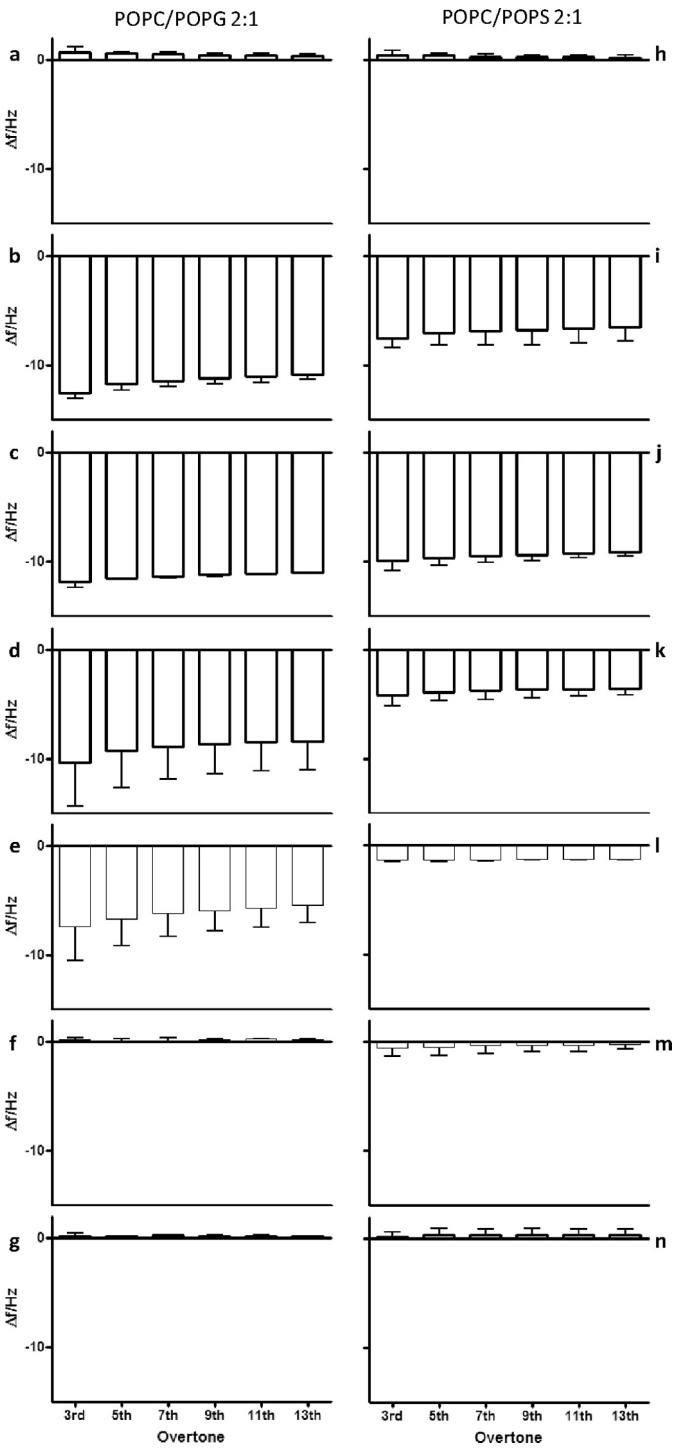

FIGURE 4. **Summary of values of Δ*f* for the 3rd, 5th, 7th, 9th, 11th, and 13th overtones derived from QCM-D measurements of supported lipid bilayers in 50 mM sodium acetate, 100 mM sodium chloride, pH 5.** The *graphs* show the change in Δ*f* induced by the addition of synthetic peptides derived from the N terminus of mouse *a* and *h,* PrP: PrP(23–50); *b* and *i,* PrP(23–89); *c* and *j,* PrP(23–110); *d* and *k,* PrP(23–110)Δ51–89; *e* and *l,* PrP(50–110); *f* and *m,* PrP(51–89); *g* and *n,* PrP(90–110) interacting with supported composite lipid bilayers consisting of (2:1) POPS/POPS (*a–g*) or POPC/POPG (*h–n*). Greater negative values indicate a larger deposit of mass to the QCM chip. Data are shown as the mean of three experiments ± S.E.

rates of motion of the headgroup (50). The width of the ^{31}P powder pattern indicates the phase of the lipids, with broader components corresponding to greater order, and narrow com-

TABLE 1

Lipid/peptide binding ratios for various synthetic peptides based on the N terminus of mouse PrP

Binding was to support composite lipid bilayers. Ratios are calculated from QCM-D measurements as the ratio between Δf upon lipid deposition and bilayer formation, to Δf associated with peptide addition. Values are the mean ± S.D. number of lipid molecules (POPC and POPG or POPS) associated with the binding of one peptide molecule. All experiments were performed in 50 mM acetate buffer, 130 mM NaCl, pH 5.

	Total lipid/peptide molar binding ratios			
	POPC/POPS, 2:1		POPC/POPG, 2:1	
PrP(23–89)	16.6	±4.0	9.8	±0.4
PrP(23–110)	15.2	±0.9	13.3	±0.3
PrP(23–110)Δ51–89	21.8	±1.9	10.7	±3.1
PrP(50–110)	79.1	±3.7	18.0	±5.6

TABLE 2

"On" (k_{on}) and "off" (k_{off}) rate constants and dissociation constants (k_d) for the association of synthetic peptides (based on the N terminus of mouse PrP) to supported composite lipid bilayers, calculated from QCM-D measurements

k_{off} was first calculated by fitting a exponential function to the dissociation phase of the QCM-D experiment. k_{on} was then calculated using the method of Christ *et al.* (42) by substituting the value of k_{off} into a binding function. Values are given as the means ± S.D. of three experiments. All experiments were performed in 50 mM acetate buffer, 130 mM NaCl, pH 5.

	Kinetic and thermodynamic lipid/peptide binding constants		
	k_{on}	k_{off}	k_d
	$M^{-1}s^{-1}$	s^{-1}	nM
POPC-POPS (2:1)			
PrP(23–89)	35,000 ± 20,000	0.005 ± 0.004	100 ± 200
PrP(23–110)	38,000 ± 23,000	0.003 ± 0.003	100 ± 140
PrP(23–110)Δ51–89	4300 ± 15,000	0.005 ± 0.001	100 ± 100
PrP(50–110)	8000 ± 10,000	0.004 ± 0.006	500 ± 600
POPC-POPG (2:1)			
PrP(23–89)	40,900 ± 21,000	0.004 ± 0.002	100 ± 70
PrP(23–110)	41,300 ± 5000	0.004 ± 0.001	100 ± 280
PrP(23–110)Δ51–89	53,000 ± 41,000	0.003 ± 0.003	100 ± 80
PrP(50–110)	54,300 ± 27,000	0.006 ± 0	120 ± 0

ponents indicate highly mobile species such as micelles undergoing isotropic motion. In contrast with the broad line ^{2}H of acyl chains, ^{31}P NMR allows differentiation between different phospholipid populations by changes in the chemical shift of the membrane components (40).

The spectra in Fig. 5 are of POPC/POPS mixtures with and without PrP(23–89) and PrP(23–110) peptides. All of the spectra have a ^{31}P powder pattern consistent with the lipids forming homogeneous lamellar bilayer vesicles. The chemical shift anisotropy (CSA) of the ^{31}P signal is related to distance between the outer edges of the powder pattern; the results are summarized in Table 3. The addition of the PrP(23–89) and PrP(23–110) peptides caused a slight increase in the ^{31}P CSA from 42.2 to 44.5 and 43.7 ppm, respectively. An increase in CSA indicates that the phospholipid headgroups undergo less extensive motions in the presence of the peptides, although the change is small, suggesting a weak interaction with the headgroup. The lack of a second CSA in the ^{31}P spectra with the peptides indicates that the peptide interaction does not cause phase separation of the POPC and anionic lipids.

^{2}H Solid-state NMR—Broad line ^{2}H NMR of chain deuterated phospholipids is a method of probing the order of the acyl chains in phospholipid bilayers. The technique probes the environment within the core of the lipid bilayer, with greater splitting between the wings of the ^{2}H spectrum correlating with greater order of the chains within the membrane. We utilized the $^2H_{31}$-palmitoyl chain of POPC to act as the probe of the bilayer. Fig. 6 shows the ^{2}H solid-state NMR spectra of MLV with and without PrP(23–89) and PrP(23–110). The spectra show that the peptides increased the outer ^{2}H splittings from 23.5 kHz for the POPC/POPS

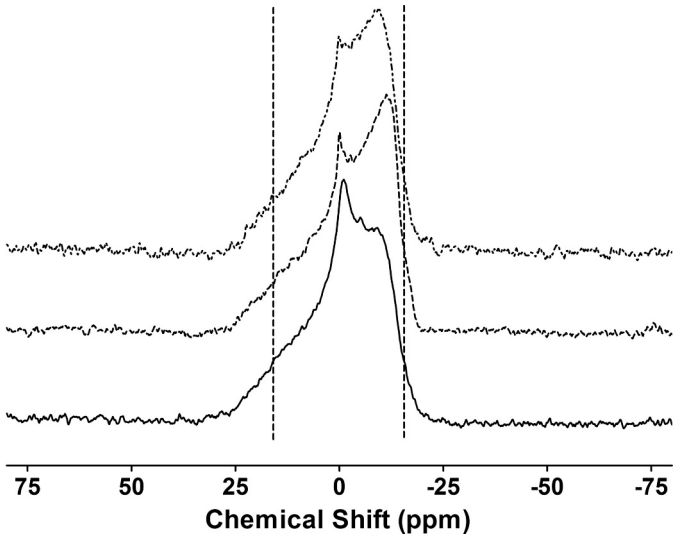

FIGURE 5. **^{31}P broad line solid-state NMR spectra of MLV composed of dPOPC/POPS (2:1) suspended in MES buffer (10 mM, pH 5) with 50 mM NaCl.** The spectra are the accumulation of 25,000 transients processed with a line broadening function of 50 Hz. *Bottom solid line* represents the lipids alone; the *middle dashed line* represents the lipids plus PrP(23–89), and the *top dot-dash line* represents the lipids plus PrP(23–110). CSA values are summarized in Table 3. The *vertical lines* are not representative and are added to aid the reader.

(2:1) MLV to 25.6 and 24.3 kHz with PrP(23–89) or PrP(23–110), respectively. The changes indicate an ordering of the lipid acyl chains by the peptides, with PrP(23–89) causing a greater increase than PrP(23–110). The ordering of the acyl chains is consistent with the QCM-D experiments, suggesting that the peptides insert deeply into the membrane core and may be entirely transmembrane. The more defined split-

TABLE 3

Effect of PrP(23–89) and PrP(23–110) on the ^{2}H and ^{31}P broad line solid-state NMR spectra and ^{31}P MAS solid-state NMR experiment relaxation times of dPOPC-POPS (2:1), pH 5

CSA and quadrupolar splitting values increase when motion within the detected group decreases, in this case both the headgroups and acyl chains are only weakly affected by the presence of the peptides.

	^{31}P CSA (±1 ppm)	^{2}H CSA (±0.1 kHz)	T_1 relaxation	T_2 relaxation
			s	*ms*
POPC-POPS	−42	23.2	0.34(±0.01)	5.3(±0.1)
+PRP(23–89)	−44	25.6	0.27(±0.01)	7.5(±0.1)
+PrP(23–110)	−44	24.4	0.27(±0.01)	9.9(±0.1)

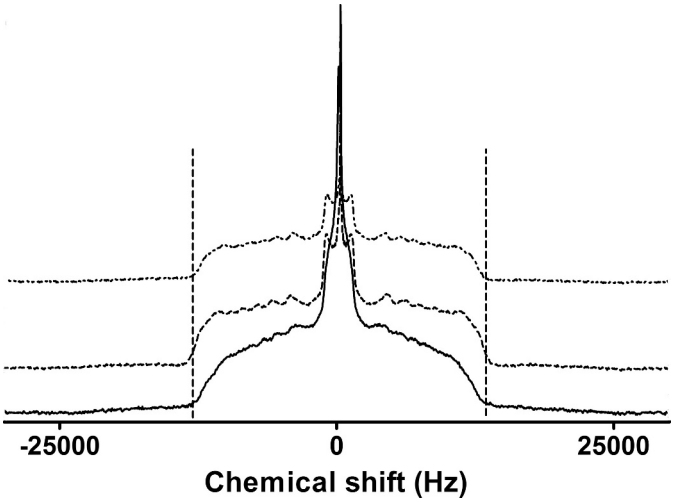

FIGURE 6. **^{2}H broad line solid-state NMR spectra of MLV composed of dPOPC/POPS (2:1) suspended in MES buffer (10 mM pH 5) with 50 mM NaCl.** The spectra are the accumulation of 250,000 transients processed with a line broadening function of 100 Hz. *Bottom solid line* represents the lipids alone; the *middle dashed line* represents the lipids plus PrP(23–89), and the *top dot-dash line* represents the lipids plus PrP(23–110). Quadrupolar splitting values are summarized in Table 3. The *vertical lines* act as an aid to the eye indicating the similarity between the outer edge of the ^{2}H spectrum with and without PrP(23–89) or PrP(23–110).

tings seen in the spectra of the MLV with peptides is due to a change in the dynamics of acyl chains, which would also suggest the peptides interact strongly with the membrane core.

^{31}P Solid-state NMR Relaxation—The ^{31}P MAS NMR longitudinal and transverse relaxation time constants (T_1 and T_2) are presented in Table 3. To determine values for T_1 and T_2, an exponential function was fitted to the intensity (integrals) of the ^{31}P NMR spectra. The spectra showed a single peak, indicating that the presence of the peptides does not lead to the formation of separate peptide bound and unbound lipid populations.

The T_1 or longitudinal ^{31}P NMR relaxation time constant for the phospholipid MLV was 338 ms. Following addition of the PrP(23–89) and PrP(23–110) peptides, the relaxation time constants decreased to 268 and 271 ms, respectively. Because T_1 reports on faster lipid headgroup motions, such as long axis rotation, the changes indicate the peptides cause the lipids to slow on the microsecond-nanosecond time scale (51). The spin-spin (T_2) NMR relaxation time constants also were determined by fitting a single exponential to the ^{31}P NMR signal. The T_2 of the MLV increased from 5.3 to 7.5 ms with PrP(23–89) and 9.9 ms with the PrP(23–110). These values are consistent with the increase in the ^{2}H order parameter and suggest that both peptides have a similar effect on rates of slower motions of the lipids, for example lateral translation.

Circular Dichroism—The peptide with the highest overall anionic membrane affinity as shown by fluorescence spectroscopy and QCM-D was studied using CD to determine whether membrane lipid binding induced changes in secondary structure. We have previously demonstrated (26) that PrP(23–89) is primarily random coil in solution at both pH 7.4 and 5. After addition of a 100-fold molar excess of the lipid mixture, 1-(9*Z*-octadecenoyl)-*sn*-glycero-3-phosphocholine (LPC) and 1-(9*Z*-octadecenoyl)-*sn*-glycero-3-phospho-L-serine (LPS) (2:1), no significant change in the CD spectrum was observed at pH 7.4 (Fig. 7*A*). However, at pH 5, the addition of LPC/LPS led to a significant change in the CD spectrum (Fig. 7*B*). The shift in negative intensity from below 200 nm to around 205 nm and increased intensity between 210 and 225 nm suggests that the presence of the lipid caused the peptide backbone to adopt a more ordered secondary structure.

DISCUSSION

Fundamental questions in relation to the normal function of PrP^{C} and the principal pathogenic pathways involved in prion disease remain unanswered, although the lipid membrane has been implicated in both roles (4). The residence of PrP^{C} within lipid rafts and the number of reported binding partners in this topographical context support the likely importance of these specialized plasmalemma microdomains in the cellular biology of the prion protein (4, 52). Much less explored has been the role of non-lipid raft domains, a consideration underscored by the endogenous trafficking and internalization route followed by PrP^{C}, especially in response to complexing of copper. Furthermore, recent studies have shown that the constitutive endoproteolytic fragments N1 and N2 both harbor intrinsic neuroprotective properties when delivered exogenously to physiologically stressed cells (26). The precise site of generation and mechanism of action of these N-terminal fragments have yet to be determined, and although intact lipid rafts appear to play at least some part in relation to the protective effects of N1/C1 cleavage (27), it is quite plausible that non-raft environments may also be important components. To further explore such possibilities, we undertook a series of experiments, with our studies providing a number of novel insights into the determinants and structural basis of the binding of PrP N-terminal peptides with non-DRM lipid membranes, especially in relation to those equivalent to the N1 and N2 fragments.

The peptides we studied were chosen to exploit the compositionally distinct regions of the N terminus, to determine the relative contribution of each in isolation, and in various combinations, to binding to synthetic non-raft membranes. Our

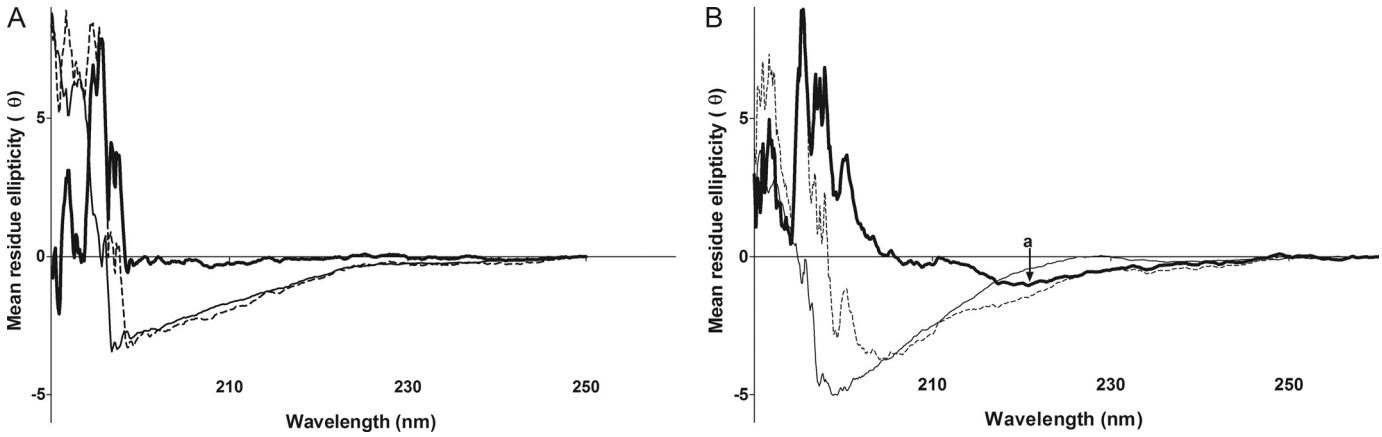

FIGURE 7. **CD spectra of PrP(23–89) in the following: *A,* in phosphate buffer, pH 7.4, without (*thin solid line*) and with (*dashed line*) LPC/LPS (2:1) with the *thick solid line* representing the difference between the two spectra; *B,* in acetate buffer, pH 5, without (*thin solid line*) and with (*dashed line*) LPC/LPS (2:1) with the *thick solid line* representing the difference between the two spectra.** The point (*a*) indicated in *B* indicates the difference in the CD spectra around 220 nm, suggesting PrP(23–89) assumes a greater proportion of β-sheet structure in the presence of lipid. The peptide/lipid molar ratio was 1:100.

QCM-D and fluorescence results were entirely congruent, with PrP(23–89) and PrP(23–110) showing the greatest binding to supported bilayers, whereas the constituent peptides (PrP(23–50), PrP(51–89), and PrP90–110) showed no binding, and PrP(50–110) and PrP(23–110)Δ51–89 displayed intermediate association. Although consistent with previous results (53), the lack of binding of the terminal region (PrP(23–50)), especially to the anionic lipids phosphatidylserine and phosphatidylglycerol, is somewhat unexpected given the high concentration of lysine residues that are positively charged at neutral pH. Our results also revealed that the octapeptide repeat region alone does not directly bind to planar lipid bilayers, indicating that a combination of the octapeptide repeat and either of the two polybasic regions (23–50 or 90–110) is needed for effective membrane interaction. These observations suggest another insight into the relevance of the evolutionary conservation of constitutive processing of PrP, which has preserved N-terminal fragments (N1 and N2) harboring at least both of these component regions.

As alluded, we believe it is noteworthy that of all the possible constituent peptide combinations assessed, the highest membrane affinity observed was for peptides equivalent to N1 and N2. Despite hypothetical considerations suggesting that each of the octapeptide repeat and polybasic regions alone could bind to anionic lipid membranes, our results suggest a synergy is required between the individual peptide segments for this to occur, which is especially prominent for the 23–50 polybasic region when combined with the octapeptide repeat domain. The precise physicochemical basis for this synergism and the structural form of the bound peptide remain to be determined. Previous work from our group has also shown the PrP(23–50) peptide to have only very limited ability to associate with lipid membranes despite mediating cytoprotective effects (26). We find the negligible membrane binding of PrP(23–50) somewhat counterintuitive given the theoretical potential for electrostatic interactions between the seven amino groups in this region to drive anionic membrane association. Nevertheless, our salt titration experiments suggest that electrostatic forces are unlikely to be operating in the membrane association of peptides containing the 23–50 segment. Regarding the octapeptide repeat domain, Raman spectroscopy studies of PrP-Cu^{II} binding suggest that at pH 5, the histidine residues of PrP will exist in a mixture of the protonated and unprotonated copper-binding states (54). As unprotonated histidine has a slight hydrophobic character, it could be speculated that the octapeptide repeat would take on this hydrophobicity because of the combination of several hydrophobic residues per repeat (proline, tryptophan, and histidine) broken only by a single hydrophilic residue (glutamine), with this characteristic serving to facilitate membrane insertion of peptides harboring this domain. Nevertheless, as for PrP(23–50), the octapeptide repeat segment alone did not bind to our synthetic membranes demonstrating that the combination of hydrophobic and polar driving forces is apparently critical to this type of lipid binding. The presence of some membrane interaction by PrP(23–110)Δ51–89 suggests that the number of repeats required to facilitate binding may be as few as one.

As described, contrary to previous claims (55), we found the octapeptide segment alone is not sufficient to drive binding to contiguous lipid membranes. Dong *et al.* (55) reported that binding of the octapeptide region to dodecylphosphocholine micelles may be driven by insertion of the tryptophan residues into the acyl chain region of the membrane. However, this region may not be as accessible in a less tightly curved membrane structure such as LUV or a cellular membrane. Furthermore, from our studies, it is clear that the N terminus does not drive binding to predominantly phosphatidylcholine membranes, as would be found in the exoplasmic face of nonstressed cellular and neuronal membranes (30). In fact, contrary to Morillas *et al.* (30), we did not observe binding at either higher pH or at lower anionic lipid ratios. Our results suggest that, even at acid pH, the N1 and N2 fragments of PrP will not directly interact with the bulk lipid of the cell membrane in the synaptic cleft without the presence of a cofactor. Conversely, the results suggest the peptides will interact directly with the cell membrane under acidic conditions similar to those found in endocytic compartments if anionic phospholipids such as phosphatidylserine are present in significant amounts (56).

In addition to facilitating a greater understanding of the determinants of non-DRM membrane binding of the N terminus of PrP, our results have also provided important new insights into the structural basis of these interactions. All peptides that bound to the lipids affected all of the QCM harmonics equally, suggesting membrane insertion rather than surface association. Furthermore, solid-state NMR of the membrane interaction of the highest affinity peptides, equivalent to the biologically relevant N1 and N2 fragments, indicated that the peptides bind by inserting into the lipid bilayer but in a minimally disruptive manner. The ^{31}P and ^{2}H solid-state NMR data indicate that the peptides insert into the membrane without strong interactions with the headgroup region, with the small increase in the order of the acyl chains showing that the presence of the peptide does not substantially perturb the freedom of motion of the palmitoyl acyl chains of POPC. Static and MAS ^{31}P experiments showed only a single peak, supporting the contention that the addition of N1 and N2 peptides did not cause a separation of the lipids into distinct micro-domains. The NMR data also showed that PrP(23–89) and PrP(23–110) have similar effects on the phospholipid membrane despite the considerably greater length of the peptide equivalent to N1. In addition, CD demonstrated a structural change in PrP(23–89) because of interaction with phosphatidylserine lipids, with a change from exclusively random coil to a significant portion of β-sheet structure.

Clearly, our results suggest that the N terminus of PrP does not interact directly with the bulk of the lipid membrane under unperturbed cell surface conditions. In contrast to previous results of wild type PrP with SUV, interactions in our studies were only seen at acidic pH, with similar pH dependence reported previously (30). Given the number of potential binding partners reported for PrP^C while in lipid rafts (7, 10, 29), the neutral pH usually present at the synaptic cleft appears to add further support for the reduced likelihood of a direct membrane interaction at this specific location. Nevertheless, as a corollary, a model is proposed to try to summarily contextualize many of our key findings, focusing on the interaction of the N terminus with membrane regions containing high concentrations of phosphatidylserine in conjunction with acidic pH. Under conditions of heightened oxidative stress, especially peroxidation of the lipid membrane as reported to occur in prion disease (57), a neuroprotective response is elicited that encompasses PrP^C while resident as a GPI-anchored protein in lipid rafts (58). As the protective response evolves, perhaps as a requisite for eliciting specific signaling cascades (59), PrP^C moves from lipid raft domains into the early endosome compartment. Simultaneously, the ATP-dependent enzyme aminophospholipid transferase, responsible for maintaining the normal membrane asymmetry of the lipid phosphatidylserine (60), is inhibited by lipid peroxidation (61), leading to increased expression of phosphatidylserine in the external leaflet of the plasmalemma, which is generally envisaged as an early marker of apoptosis (62), although other functional implications have been suggested (63, 64). Surface expression of phosphatidylserine is not in itself sufficient to inevitably cause a cell to enter apoptosis (64), and surface expression of this moiety is reversible (65) and nonhomogeneous, with regions showing disproportionately higher concentrations (47), perhaps reaching the ratios used in our study. Once trafficked, the acidic pH of the early endosome would favor the loss of any histidine-bound copper associated with PrP^C and concomitantly provide a milieu more favorable to the N-terminal binding to recently externalized phosphatidylserine, with this organelle shown to be enriched in this lipid and thereby offering a potentially important cationic protein sorting capacity (47). Endoproteolytic cleavage of PrP^C could occur at some point along this pathway and facilitate binding of liberated fragments to phosphatidylserine, but the absence of proteolysis may not preclude functionally significant binding of full-length PrP^C. Although our model is more aligned to the postulate that binding of the N terminus of PrP^C, or cognate fragments, to phosphatidylserine may serve to consolidate or promote a neuroprotective response, we cannot exclude the possibility that the loss of membrane asymmetry may serve to attenuate or abrogate PrP^C function through sequestration akin to N-terminal "tethering" (52) or perhaps indirectly such as through generic inhibition of endocytosis (67).

The peptides we studied showed a subtle but consistently higher affinity for PG- compared with PS-containing lipids. Lipids containing these headgroups have significantly different distributions within the cell with PG predominating in mitochondria. Recently, recombinant PrP has been converted into *de novo* infectious prions in association with RNA and POPG (66). Whether the differences in affinity of the N terminus of PrP for PS- and PG-containing membranes, in association with RNA, suggest a role for this region in the propagation of infection *in vivo* remains to be explored.

Acknowledgments—We thank Denis Scanlon and John Karas for their technical expertise and discussions in relation to peptide design and synthesis.

REFERENCES

1. Johnson, R. T. (2005) *Lancet Neurol.* **4,** 635–642
2. Prusiner, S. B. (1982) *Science* **216,** 136–144
3. Stahl, N., Borchelt, D. R., Hsiao, K., and Prusiner, S. B. (1987) *Cell* **51,** 229–240
4. Walmsley, A. R., Zeng, F., and Hooper, N. M. (2003) *J. Biol. Chem.* **278,** 37241–37248
5. Baron, G. S., and Caughey, B. (2003) *J. Biol. Chem.* **278,** 14883–14892
6. Hornemann, S., Korth, C., Oesch, B., Riek, R., Wider, G., Wüthrich, K., and Glockshuber, R. (1997) *FEBS Lett.* **413,** 277–281
7. Pan, T., Wong, B. S., Liu, T., Li, R., Petersen, R. B., and Sy, M. S. (2002) *Biochem. J.* **368,** 81–90
8. Viles, J. H., Cohen, F. E., Prusiner, S. B., Goodin, D. B., Wright, P. E., and Dyson, H. J. (1999) *Proc. Natl. Acad. Sci. U.S.A.* **96,** 2042–2047
9. Jones, C. E., Abdelraheim, S. R., Brown, D. R., and Viles, J. H. (2004) *J. Biol. Chem.* **279,** 32018–32027
10. Díaz-Nido, J., Wandosell, F., and Avila, J. (2002) *Peptides* **23,** 1323–1332
11. Pauly, P. C., and Harris, D. A. (1998) *J. Biol. Chem.* **273,** 33107–33110
12. Brown, L. R., and Harris, D. A. (2003) *J. Neurochem.* **87,** 353–363
13. Shyng, S. L., Heuser, J. E., and Harris, D. A. (1994) *J. Cell Biol.* **125,** 1239–1250
14. Taylor, D. R., Watt, N. T., Perera, W. S., and Hooper, N. M. (2005) *J. Cell Sci.* **118,** 5141–5153
15. Sunyach, C., Jen, A., Deng, J., Fitzgerald, K. T., Frobert, Y., Grassi, J., McCaffrey, M. W., and Morris, R. (2003) *EMBO J.* **22,** 3591–3601
16. Parkin, E. T., Watt, N. T., Turner, A. J., and Hooper, N. M. (2004) *J. Biol.*

Chem. **279,** 11170–11178
17. Caughey, B., Race, R. E., Ernst, D., Buchmeier, M. J., and Chesebro, B. (1989) *J. Virol.* **63,** 175–181
18. Harris, D. A., Huber, M. T., van Dijken, P., Shyng, S. L., Chait, B. T., and Wang, R. (1993) *Biochemistry* **32,** 1009–1016
19. Chen, S. G., Teplow, D. B., Parchi, P., Teller, J. K., Gambetti, P., and Autilio-Gambetti, L. (1995) *J. Biol. Chem.* **270,** 19173–19180
20. Deleault, N. R., Lucassen, R. W., and Supattapone, S. (2003) *Nature* **425,** 717–720
21. Wong, B. S., Chen, S. G., Colucci, M., Xie, Z., Pan, T., Liu, T., Li, R., Gambetti, P., Sy, M. S., and Brown, D. R. (2001) *J. Neurochem.* **78,** 1400–1408
22. Caughey, B., and Raymond, G. J. (1993) *J. Virol.* **67,** 643–650
23. Wang, F., Yang, F., Hu, Y., Wang, X., Wang, X., Jin, C., and Ma, J. (2007) *Biochemistry* **46,** 7045–7053
24. Kazlauskaite, J., Sanghera, N., Sylvester, I., Vénien-Bryan, C., and Pinheiro, T. J. (2003) *Biochemistry* **42,** 3295–3304
25. Wang, X., Wang, F., Arterburn, L., Wollmann, R., and Ma, J. (2006) *J. Biol. Chem.* **281,** 13559–13565
26. Haigh, C. L., Drew, S. C., Boland, M. P., Masters, C. L., Barnham, K. J., Lawson, V. A., and Collins, S. J. (2009) *J. Cell Sci.* **122,** 1518–1528
27. Haigh, C. L., Lewis, V. A., Vella, L. J., Masters, C. L., Hill, A. F., Lawson, V. A., and Collins, S. J. (2009) *Cell Res.* **19,** 1062–1078
28. Mouillet-Richard, S., Ermonval, M., Chebassier, C., Laplanche, J. L., Lehmann, S., Launay, J. M., and Kellermann, O. (2000) *Science* **289,** 1925–1928
29. Gauczynski, S., Peyrin, J. M., Haïk, S., Leucht, C., Hundt, C., Rieger, R., Krasemann, S., Deslys, J. P., Dormont, D., Lasmézas, C. I., and Weiss, S. (2001) *EMBO J.* **20,** 5863–5875
30. Morillas, M., Swietnicki, W., Gambetti, P., and Surewicz, W. K. (1999) *J. Biol. Chem.* **274,** 36859–36865
31. Re, F., Sesana, S., Barbiroli, A., Bonomi, F., Cazzaniga, E., Lonati, E., Bulbarelli, A., and Masserini, M. (2008) *FEBS Lett.* **582,** 215–220
32. Ghosh, S., Strum, J. C., Sciorra, V. A., Daniel, L., and Bell, R. M. (1996) *J. Biol. Chem.* **271,** 8472–8480
33. Fadok, V. A., Voelker, D. R., Campbell, P. A., Cohen, J. J., Bratton, D. L., and Henson, P. M. (1992) *J. Immunol.* **148,** 2207–2216
34. van den Eijnde, S. M., van den Hoff, M. J., Reutelingsperger, C. P., van Heerde, W. L., Henfling, M. E., Vermeij-Keers, C., Schutte, B., Borgers, M., and Ramaekers, F. C. (2001) *J. Cell Sci.* **114,** 3631–3642
35. Kenis, H., van Genderen, H., Bennaghmouch, A., Rinia, H. A., Frederik, P., Narula, J., Hofstra, L., and Reutelingsperger, C. P. (2004) *J. Biol. Chem.* **279,** 52623–52629
36. Farge, E., (1995) *Biophys. J.* **69,** 2501–2506
37. Coleman, B. M., Nisbet, R. M., Han, S., Cappai, R., Hatters, D. M., and Hill, A. F. (2009) *Biochem. Biophys. Res. Commun.* **380,** 564–568
38. Lau, T. L., Gehman, J. D., Wade, J. D., Perez, K., Masters, C. L., Barnham, K. J., and Separovic, F. (2007) *Biochim. Biophys. Acta* **1768,** 2400–2408
39. Koenig, B. W., Kruger, S., Orts, W. J., Majkrzak, C. F., Berk, N. F., Silverton, J. V., and Gawrisch, K. (1996) *Langmuir* **12,** 1343–1350
40. Pukala, T. L., Boland, M. P., Gehman, J. D., Kuhn-Nentwig, L., Separovic, F., and Bowie, J. H. (2007) *Biochemistry* **46,** 3576–3585
41. Mechler, A., Praporski, S., Atmuri, K., Boland, M., Separovic, F., and Martin, L. L. (2007) *Biophys. J.* **93,** 3907–3916
42. Christ, K., Al-Kaddah, S., Wiedemann, I., Rattay, B., Sahl, H. G., and Bendas, G. (2008) *J. Membr. Biol.* **226,** 9–16
43. Ladokhin, A. S., Jayasinghe, S., and White, S. H. (2000) *Anal. Biochem.* **285,** 235–245
44. Plager, D. A., and Nelsestuen, G. L. (1994) *Biochemistry* **33,** 7005–7013
45. Murphy, E. J., and Horrocks, L. A. (1993) *Lipids* **28,** 67–71
46. Lau, T. L., Ambroggio, E. E., Tew, D. J., Cappai, R., Masters, C. L., Fidelio, G. D., Barnham, K. J., and Separovic, F. (2006) *J. Mol. Biol.* **356,** 759–770
47. Yeung, T., Gilbert, G. E., Shi, J., Silvius, J., Kapus, A., and Grinstein, S. (2008) *Science* **319,** 210–213
48. Schlame, M., Brody, S., and Hostetler, K. Y. (1993) *Eur. J. Biochem.* **212,** 727–735
49. Seelig, J. (1978) *Biochim. Biophys. Acta* **515,** 105–140
50. Dufourc, E. J., Mayer, C., Stohrer, J., Althoff, G., and Kothe, G. (1992) *Biophys. J.* **61,** 42–57
51. Separovic, F., Cornell, B., and Pace, R. (2000) *Chem. Phys. Lipids* **107,** 159–167
52. Zeng, F., Watt, N. T., Walmsley, A. R., and Hooper, N. M. (2003) *J. Neurochem.* **84,** 480–490
53. Oglecka, K., Lundberg, P., Magzoub, M., Göran Eriksson, L. E., Langel, U., and Gräslund, A (2008) *Biochim. Biophys. Acta* **1778,** 206–213
54. Miura, T., Hori-i, A., Mototani, H., and Takeuchi, H. (1999) *Biochemistry* **38,** 11560–11569
55. Dong, S. L., Cadamuro, S. A., Fiorino, F., Bertsch, U., Moroder, L., and Renner, C. (2007) *Biopolymers* **88,** 840–847
56. Murphy, R. F., Powers, S., and Cantor, C. R. (1984) *J. Cell Biol.* **98,** 1757–1762
57. Brazier, M. W., Lewis, V., Ciccotosto, G. D., Klug, G. M., Lawson, V. A., Cappai, R., Ironside, J. W., Masters, C. L., Hill, A. F., White, A. R., and Collins, S. (2006) *Brain Res. Bull.* **68,** 346–354
58. Kuwahara, C., Takeuchi, A. M., Nishimura, T., Haraguchi, K., Kubosaki, A., Matsumoto, Y., Saeki, K., Matsumoto, Y., Yokoyama, T., Itohara, S., and Onodera, T. (1999) *Nature* **400,** 225–226
59. Caetano, F. A., Lopes, M. H., Hajj, G. N., Machado, C. F., Pinto, Arantes, C., Magalhães, A. C., Vieira, Mde, P, Américo, T. A., Massensini, A. R., Priola, S. A., Vorberg, I., Gomez, M. V., Linden, R., Prado, V. F., Martins, V. R., and Prado, M. A. (2008) *J. Neurosci.* **28,** 6691–6702
60. Esterbauer, H., Schaur, R. J., and Zollner, H. (1991) *Free Radic. Biol. Med.* **11,** 81–128
61. Castegna, A., Lauderback, C. M., Mohmmad-Abdul, H., and Butterfield, D. A. (2004) *Brain Res.* **1004,** 193–197
62. Rimon, G., Bazenet, C. E., Philpott, K. L., and Rubin, L. L. (1997) *J. Neurosci. Res.* **48,** 563–570
63. Smrz, D., Dráberová, L., and Dráber, P. (2007) *J. Biol. Chem.* **282,** 10487–10497
64. Stowell, S. R., Karmakar, S., Arthur, C. M., Ju, T., Rodrigues, L. C., Riul, T. B., Dias-Baruffi, M., Miner, J., McEver, R. P., and Cummings, R. D. (2009) *Mol. Biol. Cell* **20,** 1408–1418
65. Bevers, E. M., Tilly, R. H., Senden, J. M., Comfurius, P., and Zwaal, R. F. (1989) *Biochemistry* **28,** 2382–2387
66. Wang, F., Wang, X., Yuan, C. G., and Ma, J. (2010) *Science* **327,** 1132–1135
67. Farge, E., Ojcius, D. M., Subtil, A., and Dautry-Varsat, A. (1999) *Am. J. Physiol.* **276,** C725–C733